Analysis of fracture network geometries and orientations within a fold-and-thrust structure in the Northern Apennines, Italy

M. Benthem and H.C. de Vries, 2013

Abstract

This research focuses on fracture networks in sedimentary rocks within the Umbria-Marche fold-and-thrust belt in the Northern Apennines, Italy. The aim of this research is twofold, namely to correlate the geometry of fracture networks with tectonic position and lithology and to correlate the orientation of fracture networks with the origination of a fold-and-thrust structure. The fold-and-thrust belt within the area strikes about N160° and developed in the Miocene within a compressional regime as the result of the collision between the European Corsica-Sardinia Margin and the Adriatic plate, accompanied by back-arc extension due to rollback.

In order to analyze geometries of fracture networks software named DigiFract is used to digitize outcrops in the field. Fracture orientation, density, spacing, height and termination are analysed for different lithologies within the Umbria-Marche succession.

Orientations of fracture sets are correlated to different structural stages during the development of the fold-and-trust structure. The first stage in which fractures develop is layer parallel shortening, during which bedding-normal pressure-solution surfaces develop, striking parallel to the hinge line. Subsequently, longitudinal joints striking parallel to the hinge line develop during fold initiation. This is followed by amplification and tightening of the fold, causing development of transversal joints, striking perpendicular to the hinge line.

In theory, fold limbs are preferred sites for deformation within an active-hinge fault-related anticline, rather than the corresponding anticlinal crests (Salvini and Storti, 2001; Salvini and Storti, 2004). Our data is not substantial to proof this theory, but is in accordance to it.

Chert, primarily present in the Maiolica Fm and the Diasprini Fm, and marl, present in the Bisciaro Fm, act as non-fractured or very low density-boundary between fractured beddings.

Siliclastic turbidites are less fractured than carbonates at similar tectonic positions.

Keywords: fracture network geometry, fracture orientation, fold-and-thrust structure, DigiFract software

Introduction

The presence of fractures in hydrocarbon reservoirs highly enhances permeability and thereby affects the flow in a reservoir. Therefore understanding about the geometry and orientation of fracture networks within a reservoir is of importance.

Fracture networks are typical of deformed brittle rocks, with folding as an important fracture-generating deformation mechanism (Hancock, 1985). Other influences on the development and the geometry of fracture networks are sedimentological architecture and rheology of the rock. The rheology, hence the “degree of brittleness” of a rock, is dependent on lithology when under equal boundary conditions (confining pressure, temperature, strain rate) (Dürrast and Siegesmund, 1999; Sinclair, 1980).

This research focuses on fracture networks in sedimentary rocks within a fold-and-thrust belt. The aim is twofold, namely to correlate the geometry of fracture networks with tectonic position and with lithology and to correlate the orientation of fracture networks with the origination of a fold-and-thrust structure.

The sedimentary rocks investigated include carbonate rocks from Jurassic and Triassic and sands and marls from Paleogene and Neogene.

Fieldwork is carried out in the Sibillini Mountains, the central-eastern part of the Umbria-Marche Apennines, in the region around the village of Fiastra, province of Macerata, Italy.

In order to analyze the properties of fracture networks, such as fracture density, height and termination, outcrops were digitized with computer software, called DigiFract. With use of this software, fracture properties were studied and mapped and a statistical analysis of these properties was carried out.

Research was carried out in collaboration with Steenhuisen, V., van Veen, D.J., and Alsemgeest, J., who focussed on the structural geology of the area in order to obtain constraints to the tectonic evolution of the area.

1. Geologic setting

1.1. Geologic history

The folded belts of the Apennines are derived from a small ocean and from its European and Apulian-Adriatic continental margins. This nowadays disappeared ocean is named Ligurian Tethys, which is a segment of a more extensive ocean, the Mesozoic Tethys (Lemoine, 1982).

The Mesozoic Tethys developed as a result of the breaking up of the supercontinent Pangea. Two kinematic systems acted successively during the break-up of Pangea, reflected by two main lines of disruption: a latitudinal Tethys break and a meridian Atlantic break, having in common a Central Atlantic segment (Lemoine, 1982) (Fig. 1).

Starting during the Late Jurassic, the opening of the Tethyan system led to the partition of Pangea into two major continents, Laurasia and Gondwana, with the Central Atlantic Ocean separating Africa from North America (Fig. 2a). Successively, rifting and opening of the Atlantic system occurred with a

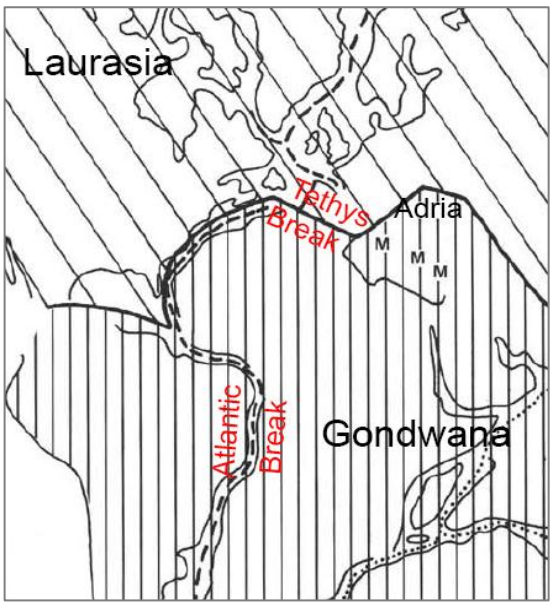

Figure 1: Tethys and Atlantic break during the end of Triassic. Broken line: Atlantic break, continuous line: Tethys break (Lemoine, 1982)

northward propagation, resulting in the opening of the South Atlantic Ocean in the Early Cretaceous (Lemoine, 1982) (Fig. 2b).

The opening of the South Atlantic Ocean caused the counter clockwise rotation of the African continent, resulting in convergence between the Adriatic plate, a promontory of the African plate, and the Eurasian plate (Gaetani M., 2010). A subduction zone between the oceanic part of the Adriatic plate and the Eurasian plate developed, resulting in a fault and thrust belt on the boundary of the Eurasian plate: the Alpine orogeny. Within this subduction zone, rollback took place, as the angle of the colder, denser oceanic crust became larger. Due to the rollback process, the actual zone of subduction retreated eastward, as well as the South-Eastern boundary of the Eurasian plate (Guenguen et al., 1997) (Fig. 4). Due to this extension within the rollback process, several irregular basins emerged, younger in age from west to east (Guenguen et al., 1997). Figure 3 shows the Middle Miocene palaeotectonic reconstruction of the western Mediterranean.

As the counter clockwise rotation of the Adriatic plate proceeds, the oceanic domain south of the Eurasian margin progressively closes. Around 25 Ma continental collision between the European Corsica-Sardinia Margin and the Adriatic plate developed the Umbria-Marche fold and thrust belt as part of the Apennine orogeny, accompanied by Tyrrhenian back-arc extension (Mazzoli et al., 2005).

Figure 2a: Palaeographic world map, Late Jurassic (Scotese, 2001)

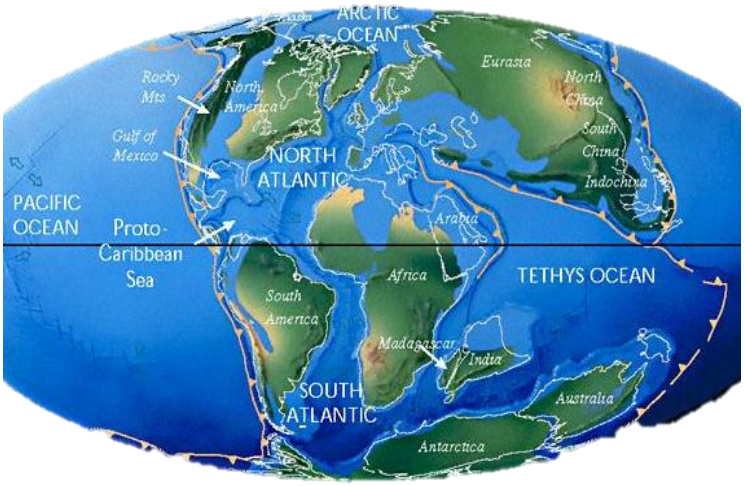

Figure 2b: Palaeographic world map, Late Cretaceous (Scotese, 2001)

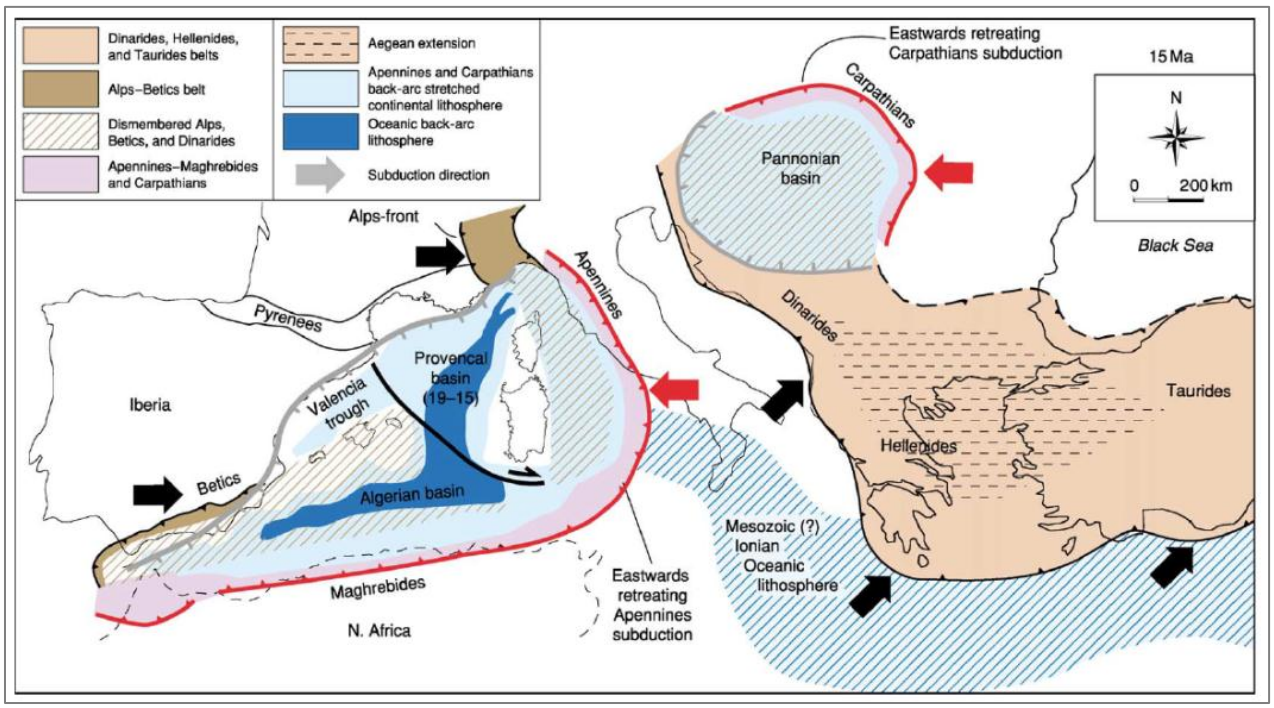

Figure 3: Palaeogeodynamics of the Mediterranean about 15 Ma (Carminati and Doglioni, 2005)

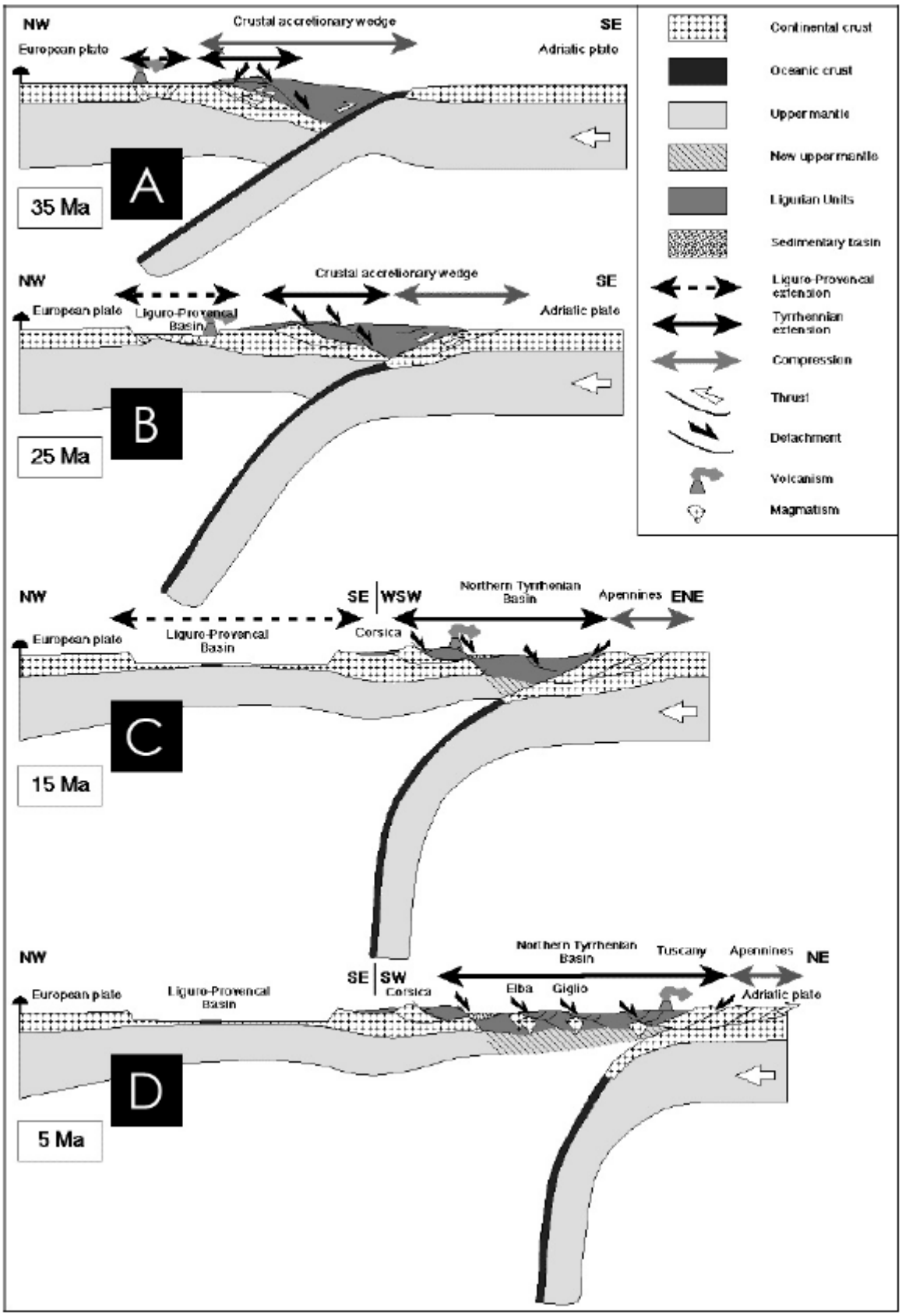

Figure 4: The evolution of the Mediterranean along the trace shown on the map (inset). On the left side, the early eastwards-directed Alpine subduction and the Apennines subduction along the Alps retrobelt are shown. Several irregular troughs, including the Tyrrhenian Sea, develop in the back arc, migrating in age from west to east (E. Gueguen et al, On the post-25 Ma geodynamic evolution of the western Mediterranean)

1.2. Lithostratigraphy

The lithostratigraphy in the study area is represented by the Umbria-Marche succession, which entirely consists of sedimentary rocks (Fig. 5).

In late Triassic, marine transgression occurred due the rifting responsible for the breaking up of Pangea. This shallow water environment resulted in the formation of the Anidriti di Burano Fm, a thick succession (1-2 km) of carbonate-evaporites deposits at the base of the Umbria-Marche succession (Di Naccio et al, 2005).

An environmental change in early Jurassic times resulted in the beginning of carbonate sedimentation in the area subjected to extension. In early Liassic times the first carbonate deposit that is now visible in the Monti Sibillini area was formed, namely the Calcare Massiccio Fm: a thick-bedded, whitish biomicrite. The thickness of the Calcare Massiccio varies between 600 and 800 meters, due to synsedimentary normal faults. During the entire Jurassic the area remained subjected to extension, whereby normal faults created horst and graben structures that controlled the deposition (Guerrera et al., 2012).

Due to propagated rifting, drowning occurred in the grabens and complete successions developed. Drowning of the horsts, on the footwall of the normal faults, cannot be explained by propagated rifting, but one of the possible reasons could be sea-level rise. After drowning, condensed succession developed on the horsts (Guerrera et al., 2012).

The condensed succession is characterized by sub-tidal to supra-tidal carbonates and shows hiatuses over time. The complete succession is composed of the Calcare Massiccio Fm, the Corniola Fm, the Bosso Fm, the Sentino Fm and the Calcari Diasprigni Fm respectively (Marchegiani et al, 1999).

In the Early Cretaceous the rifting slowed down and the Maiolica Fm was deposited, smoothing out the irregularities in the Jurassic seabed. In the Maiolica, variations in thickness are visible due to the deposition on the irregular seabed (Mazzoli et al., 2005).

From the Aptian age more marls and shales were being deposited, resulting in the Marne a Fucoidi Fm and afterwards in the Scaglia formations. Towards the top of the formation a higher amount of clay is visible, resulting in more marly limestones like the Scaglia Variegata Fm. Due to gentle tectonic activity during the Eocene, deposits of turbidite origin occur in the upper member of the Scaglia Rossa and the Scaglia Variegata Fms (Guerrera et al., 2012).

In the Early Miocene, volcanic activity resulted in the occurrence of volcanogenic material, which can be seen in the Bisciaro Fm. Also in the overlying Schlier Fm some diluted volcanogenic materials can be recognized, but this formation is mainly characterized by hemipelagic lithofacies. The deposition of the Schlier Fm is followed by typical siliciclastic turbiditic successions, including the Formazione della Laga Fm. This siliciclastic supply indicates the onset of a foredeep stage (Guerrera et al., 2012).

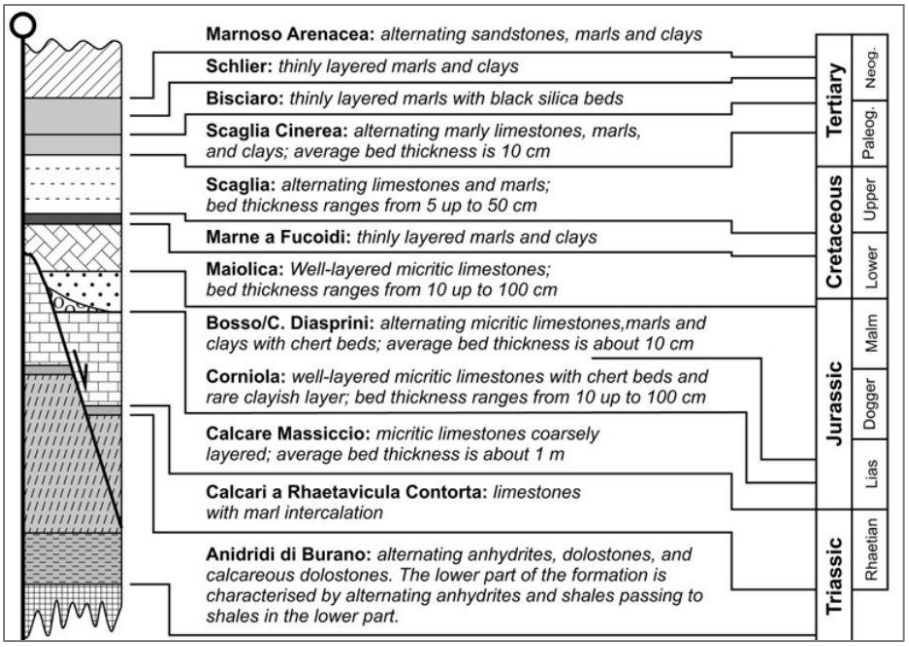

Figure 5: The Umbria-Marche succession (Tavani et al., 2008)

1.3. Present day geology

1.3.1. Umbria-Marche Apennines

The Umbria-Marche Apennines are an ENE-verging fold and thrust belt of Mio-Pliocene age (Scarselli et al., 2007), consisting of both continental crust of the European and Adriatic plates (Carminati et al., 2002).

Figure 7 shows an overview of the geology of the Apennines, our study area is denoted with a red star. West of the study area, two major extensional fault systems are present, cutting the thrust sheets: the Quarternary Monte Vettore Fault (VF in Fig. 7b) to the south, and the Monte San Vicino Fault to the north (SFV in Fig. 7b) (Tavani et al., 2012). The large normal fault systems present in the Northern Apennines are younger than the thrust sheets. Locally, extensional faults that developed in the early Jurassic during the opening of the Tethys Ocean are present, some of them reactivated in the Eocene as a result of the rollback of the subducting Adriatic plate under the Eurasian plate (Tavani et al., 2012).

1.3.2. Geology of study area

Figure 8a and 8b show a schematic overview of the geology of our study area and the geological map of the study area respectively. The locations of examined outcrops are denoted with green boxes and the Col number, as will be further discussed in Strategy. In red, the schematic cross section constructed by Tavani et al. (2012) is denoted (Fig. 9). On this cross-section, tectonic positions defined in this research are indicated, which will be further discussed in Strategy. In green, a more detailed cross section by Steenhuisen et al. (2013) is denoted (Fig. 10).

Sibillini thrust

In the study area a fold-and-thrust structure is present, striking parallel to the general Apennines strike (NNW). The main thrust is the Sibillini thrust, indicated in blue in Figure 8a. This thrust represents the trailing fault of the system responsible for the overthrusting of the mountain front and is exposed near the village of Monastero. The orientation of the fault plane of this thrust is 230/34 in our study area. Lateral shortening is established at 1800 m in our study area (Steenhuisen et al., 2013).

Anticlinal structure

In the hanging wall of the Sibillini thrust an anticlinal structure is present. This anticlinal structure has a constantly dipping backlimb (dip about 30°) with a smooth transition to the flat-lying crest. The forelimb has a variable dip and includes an overturned sector due to thrusting (Tavani et al., 2012; Steenhuisen et al., 2013).

The backlimb of this anticlinal structure is cut by a smaller thrust fault, with a corresponding anticlinal structure in its hanging wall. This thrust fault and corresponding anticline are oriented parallel to the large anticline and the Sibillini thrust and originated within the same stress regime. The fault crops out west of the village of Fiastra (Fig. 10).

Footwall

In the footwall of the Sibillini thrust, orientations indicating an anticlinal structure are found, with limbs having a maximum dip of 40° (Steenhuisen et al., 2013).

Hinge line

The hinge line of the main anticline in the hanging wall of the Sibillini thrust, denoted in orange in Figure 8a, strikes about N163° in the northern portion of the study area and N153° in the southern portion of the study area. The hinge line has a negligible plunge that never exceeds 6° (Tavani et al., 2012; Steenhuisen et al., 2013).

Extensional faults

The hanging wall of the Sibillini thrust is cut by extensional faults, striking north and dipping west. These are partially reworked inherited early Jurassic ones, as testified by thickness variation of Jurassic sediments across them (Tavani et al., 2012) (Fig. 9).

2. Data acquisition

2.1. Strategy

In order to correlate the geometry of the fracture networks with tectonic position and lithology, the fracture sets in each formation are studied at different tectonic positions.

In this research we focus on the large NNW striking anticlinal structure in the hanging wall of

the Sibillini thrust, and on differences between the hanging wall and the footwall of the Sibillini thrust.

Therefore the aim is to obtain outcrops that are not influenced by the fault damage zone of neither the Sibillini thrust nor the smaller 'Fiastra' thrust.

We defined five different tectonic positions, indicated in the schematic cross-section of the area in Figure 9.

Four tectonic positions are distinguished in the hanging wall of the Sibillini thrust: the western limb far from the fold axis, the western limb near the fold axis, the eastern limb and the overturned sector of the eastern limb. The fifth tectonic position that we examined is the footwall of the Sibillini thrust.

In total, six different formations are studied at the tectonic positions mentioned above, denoted in the matrix in Table 1. The six formations that are chosen each represent a type of rock and depositional environment. The best outcropping formations within such a rock type and depositional environment are chosen in order to obtain the most complete data set possible. Outcrops close to the cross section are preferred, in order to minimize distortion in the dataset. However, this was not always possible, no suitable outcrops for all desired combinations of lithology and tectonic position were present in the study area. For example, the Scaglia Rossa Fm occupied a large part of the surface in the area, but no suitable outcrops were present at the western limb near the fold axis.

The following formations were studied: the Calcare Massiccio Fm, the Calcare Diaspirini Fm as representative of the pelagic deposits during the rifting phase in the Jurassic, the Maiolica Fm that smoothed out the irregular seabed when the rifting slowed down at the end of the Jurassic, the Scaglia Rossa as representative of the marl and shale containing carbonates, the Bisciaro Fm representing the volcanogenic containing rocks, and finally Formazione della Laga and Formazione della Camerino which were deposited as turbidities.

Each digitized surface within an outcrop was denoted with "Col…" and digitized as described in Methodology. Some outcrops contained multiple fracture sets. When the orientation of the outcrop surface is parallel to the orientation of one of the fracture sets, this particular fracture set is badly visible. Curvature of an outcrop surface made it possible to overcome this problem and to digitize multiple fracture sets within an outcrop. Different digitized fracture sets in one outcrop are assigned to different Col numbers in this case (Fig. 6).

When apart from the digitized fracture sets in an outcrop fracture sets were present that were not suited for DigiFract, fracture orientations of these sets were measured, fracture type was defined and notes taken in the field book to be able to link these sets with other sets or stress directions later on. These 'undigitized' fracture sets are denoted with Col...a/b/etc. For example, an undigitized fracture set from which only orientations are measured within the same outcrop as digitized set 'Col 1' is denoted with 'Col 1a'.

In total, 19 outcrop surfaces were digitized. Col 11 is discarded later on because of biasing.

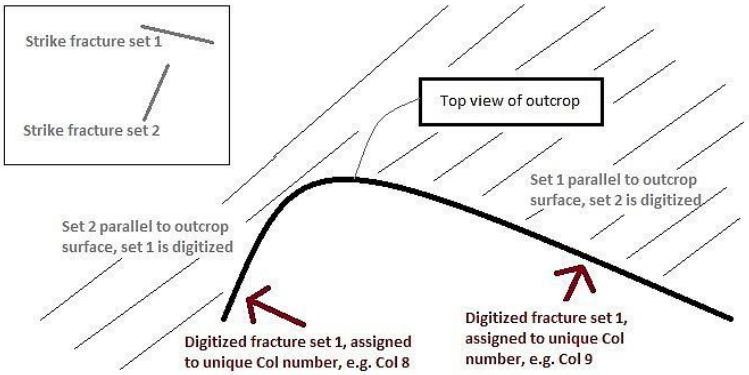

Figure 6: Curvature along an outcrop makes it possible to digitize multiple fracture sets within an outcrop

Formation	Western limb, far from fold axis	Western limb, near fold axis	Eastern limb	Eastern limb, overturned sector	Footwall
Turbidities	Col 12, Col 13				Col 18
Bisciaro	Col 2				Col 15
Scaglia Rossa	Col 14		Col 10		Col 4
Maiolica		Col 1	Col 7, Col 17	Col 16, Col 19	
Calcari Diaspirini		Col 3	Col 6		
Calcare Massiccio	Col 5	Col 8, Col 9			

Table 1: Matrix containing the digitized outcrops of formations from the Umbria-Marche succession at different tectonic positions

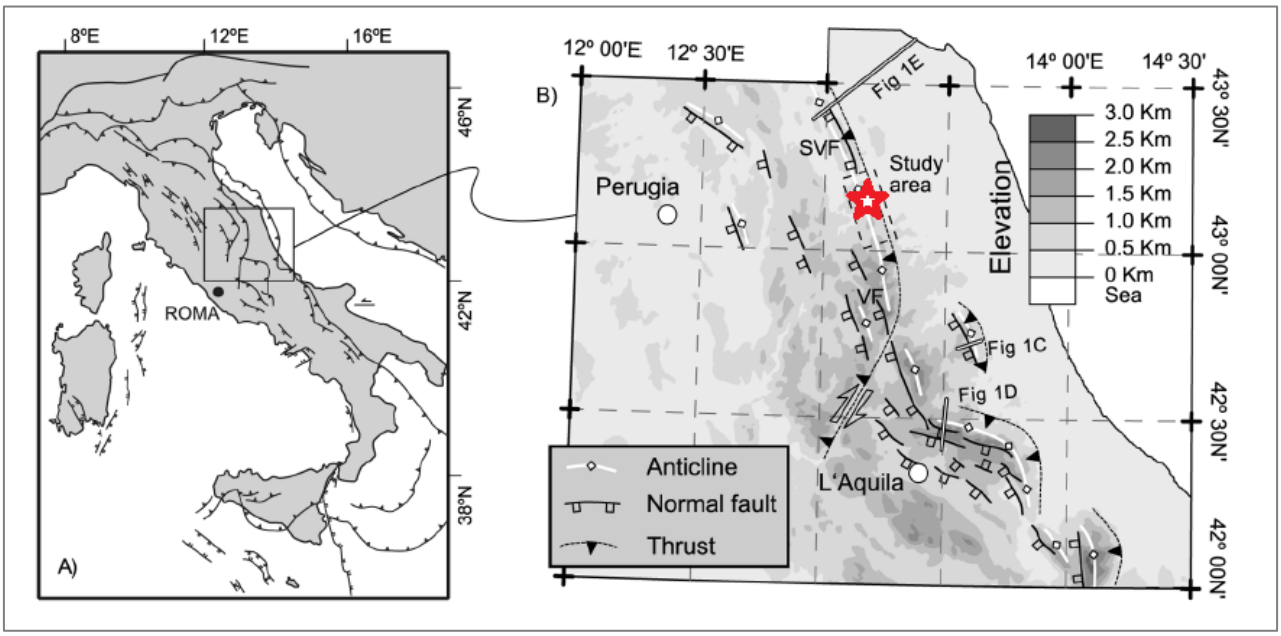

Figure 7a, 7b: Present day geological setting of Italy, including the Umbria-Marche Apennines (Tavani et al., 2012). The red star indicates our study-area

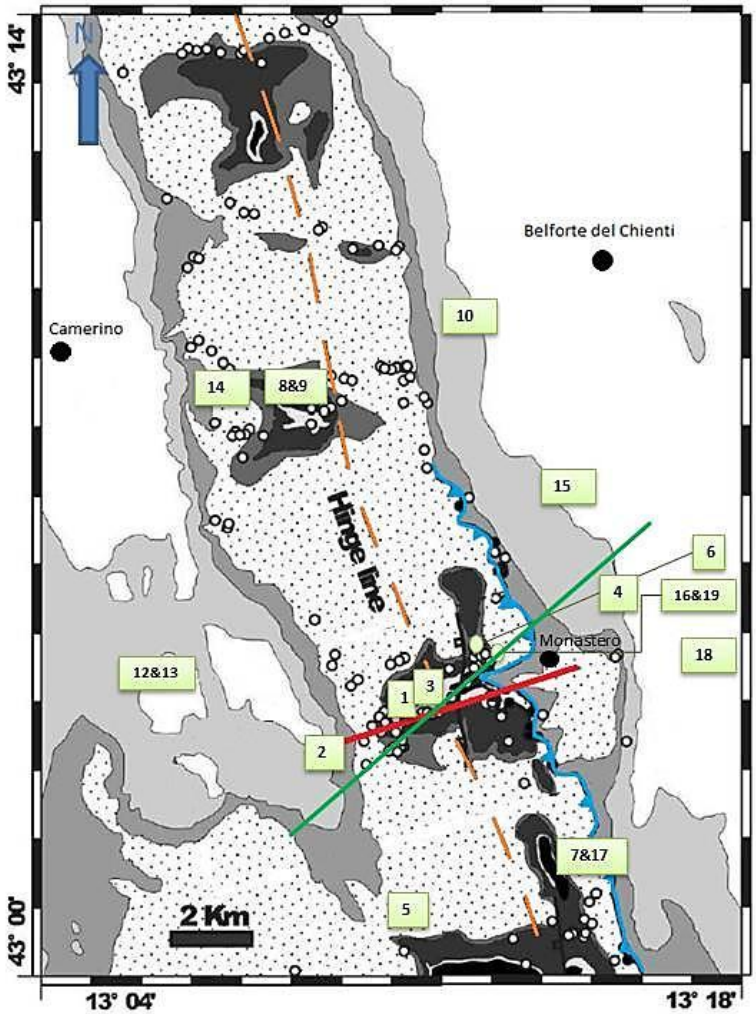

Figure 8a: Schematic overview of the geology of the study area (Tavani et al., 2012), including the positions of the outcrops digitized in DigiFract. In red the cross-section of Tavani et al. (2012) and in green the cross-section of Steenhuisen et al. (2013) are denoted. In orange, the hinge line of the main anticlinal structure in the hanging wall of the Sibillini thrust is indicated, the Sibillini thrust is indicated in blue

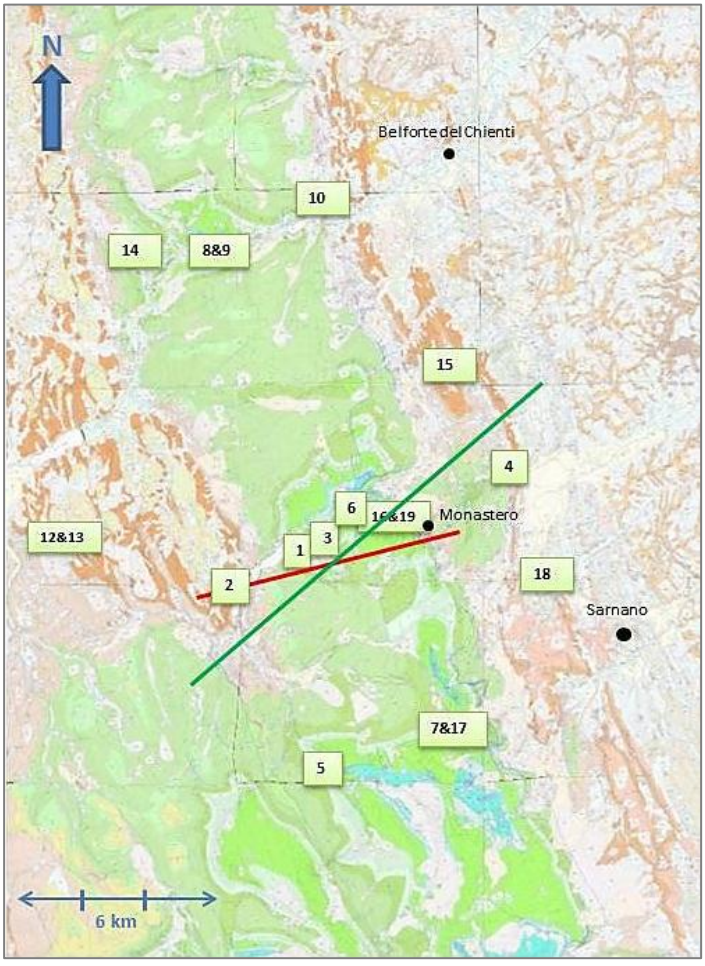

Figure 8b: Geological map of the study area, including the positions of the outcrops digitized in DigiFract. In red the cross-section of Tavani et al. (2012) and in green the cross-section of Steenhuisen et al. (2013) are denoted

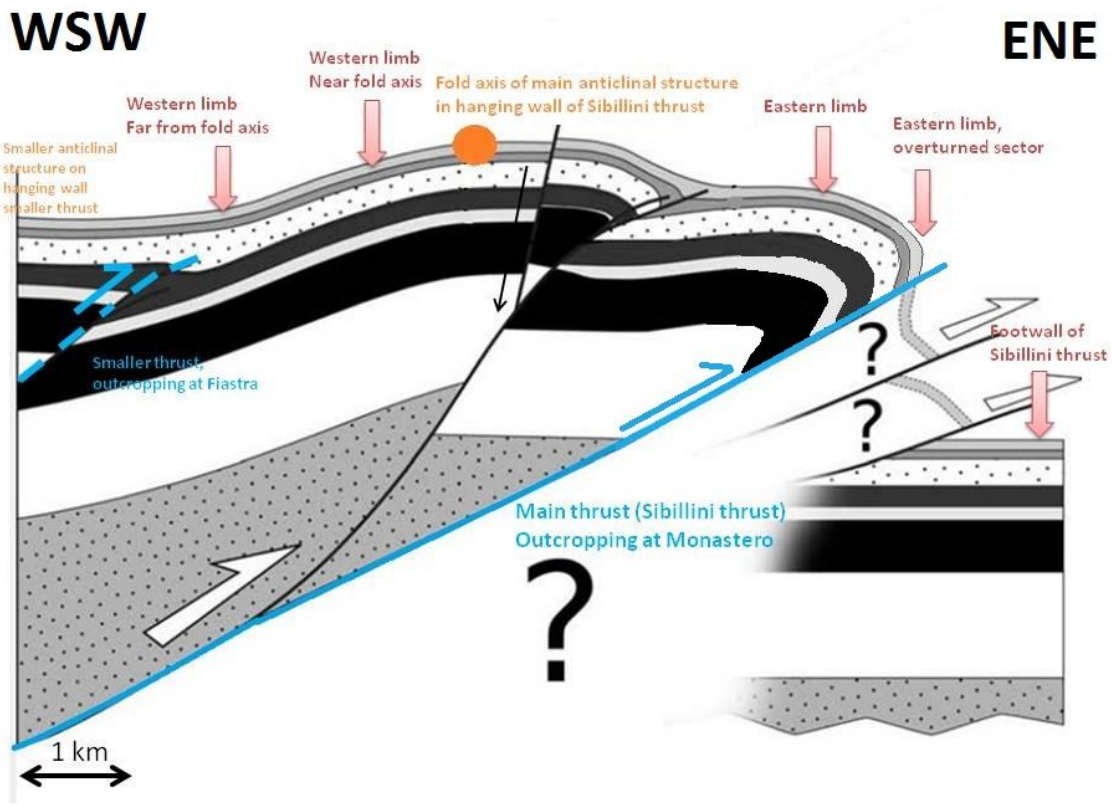

Figure 9: Schematic cross section of study area, the profile line is depicted with red in Fig. 7a and 7b (Tavani et al., 2012) Note: the footwall is not horizontal as in reality, but folded as shown in the more detailed cross-section in Figure 10.

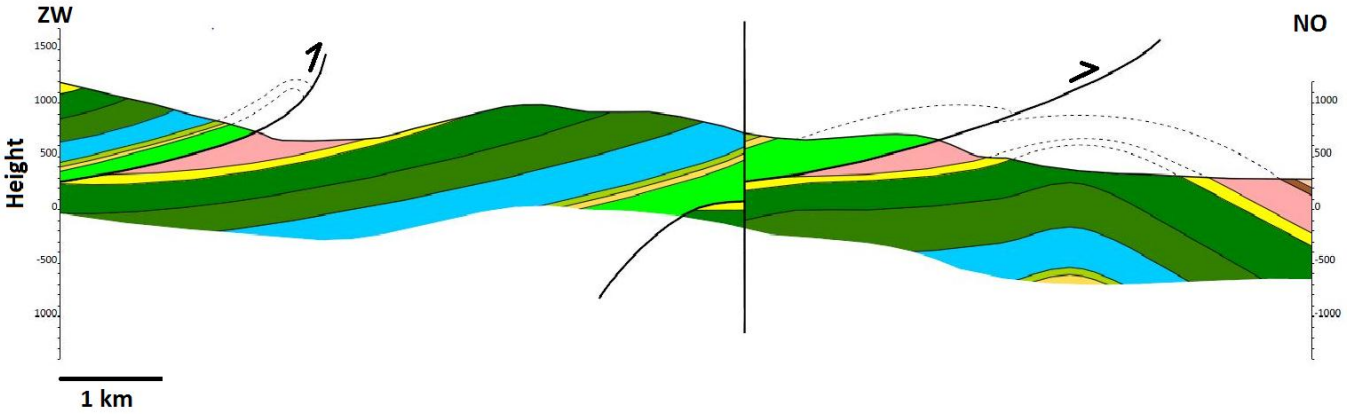

Figure 10: Detailed cross section of study area (Steenhuisen et al., 2013), the profile line is depicted with green in Figure 7a and 7b.

2.2. Methodology

2.2.1. Digitizing an outcrop

Digitizing an outcrop is done in the field by two persons, using a laptop with touchscreen with software called DigiFract (Hardebol and Bertotti, 2012).

After a representative part of the formation and the fracture set(s) within the formation is chosen, a window is defined: a part of the outcrop between circa 4 m^2 and 10 m^2 that will be digitized. A horizontal baseline is placed parallel to the outcrop, used for measurement and scaling. The orientation of the baseline is measured and entered in DigiFract later on. A photograph of the outcrop is taken, transferred to the laptop and loaded in DigiFract. The photograph is linked to a CoI with a certain position on the background map, determined with use of GPS coordinates.

Scaling is done by providing the actual length of the baseline in DigiFract. A boundary box is drawn in DigiFract to define the region of interest. If necessary, the boundary box can be adjusted later in the process. Afterwards, bedding lines are drawn and bedding orientation entered. Now the fractures can be drawn: one person stands close to the outcrop, another person is drawing the fractures on the photograph background in DigiFract, while facing the outcrop.

The person close to the outcrop precisely indicates to the person with the laptop where the fractures are, where they terminate and what the orientation of a particular fracture is.

Finally, the thickness of each layer that is digitized, the lithology, the fracture type and other observations, such as the presence of chert, are recorded in the field book.

2.2.2. Suitability of an outcrop

Each outcrop digitized must be a representative part of the formation and the fracture set(s) within the formation at a certain tectonic position. The outcrops should be accessible, in order to be able to measure the bedding and fracture orientation. Too much vegetation or weathering make an outcrop unsuited, because information becomes invisible or distorted.

To be suitable for DigiFract, an outcrop has to meet additional requirements. First of all, the view on the outcrop should be perpendicular or close to perpendicular to the horizontal to ensure little to none distortion in the photograph taken. Furthermore, bedding and fractures must be clearly displayed, i.e. from a point of view that is parallel or oblique to the strike, to obtain a data set distorted as little as possible.

Outcrops with a severe degree of deformation, often resulting in fractures with a lot of different orientations, that cross each other and a lot of other small structures such as conjugate fault sets present, are less suited for DigiFract. In these outcrops, fracture sets are often distorted and/or can often be badly distinguished from each other.

2.2.3. Processing data

Fracture density

DigiFract has the possibility to place a so-called trackline perpendicular to the bedding. A scanline, perpendicular to the trackline, scans the entire boundary box along the trackline. The scanline counts the number of fractures on the lines perpendicular to the trackline, with a resolution set to be 2 cm. The result is a detailed measurement reading along the height of the window. Subsequently, these readings are converted to three graphs, using Excel: Number of Intersects [-] vs. Height [m], Fracture Density [m^{-1}] vs. Height [m], Average Fracture Spacing [m] vs. Height [m], with the latter including an error-bar to gain insight in the reliability.

The Average Fracture Spacing [m] and the Average Fracture Height [m] are plotted in histograms.

Fracture type and orientation

The orientation of a fracture set of a certain type in combination with the orientation of the bedding and tectonic position allows us to correlate the fracture set with principal stress directions and thereby with the origination of the fold-and-thrust belt. This is possible because different types of fractures develop with a different orientation with respect to principal stresses. This will be discussed further in paragraph 3.1.2.

A difficulty that arose in processing data concerned fractures with a dip of 90° or a dip close to 90°.

With a dip that steep, dip directions easily differ 180°, thereby resulting in a data set with a wrong average and a falsely large standard deviation. For fracture sets with this problem, we determined the right dip direction at the outcrop and nullified the problem by adding 180° to the dip directions of the fractures that were applicable, to obtain a fracture set with a strike with a range of 180°.

3. Fracture Analysis

3.1. Fractures and other minor structures related to folding and thrusting

In this paragraph, observations made in the field will be linked to several structural stages during folding and thrusting. The fold which we will focus on is the large anticlinal structure in the hanging wall of the Sibillini thrust. When referring to the hinge line, the hinge line of this anticlinal structure

is meant, unless another fold structure is specifically mentioned (this hinge line is denoted in orange in Figure 8a and 9).

3.1.1. Observations

Types of fracture sets

In the study area, mode 1 fractures were found in the form of joints and stylolites. Apart from a few exceptions that will be discussed later, three groups can be distinguished. The first group concerns stylolites, which strike about parallel to the hinge line of anticlinal structure in the hanging wall of the Sibillini thrust (Fig. 11a). The second and third group concern joints, occurring with two different orientations. The first joint sets strikes about parallel to the hinge line of the anticlinal structure in the hanging wall of the Sibillini thrust (Fig. 11b), and will be denoted as longitudinal joint set further on. The other joint set strikes about perpendicular to the hinge line (Fig. 11c), and will be denoted as transversal joint set further on. Table 2 displays an overview of the three groups of fracture sets that are encountered in the study area.

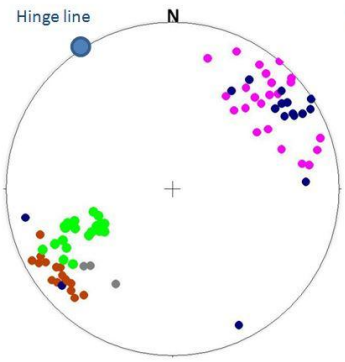

Figure 11a: Stylolites striking about **parallel to hinge line** of large anticlinal structure in hanging wall of Sibillini thrust

Violet:	Col 10a
Dark blue:	Col 14
Green:	Col 5
Brown:	Col 4
Grey:	Col 2a

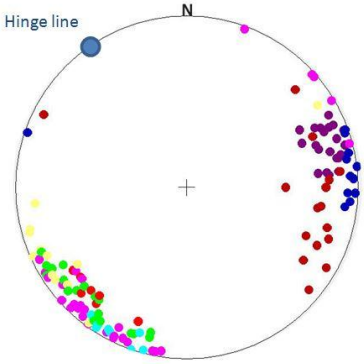

Figure 11b: Joints striking about **parallel to hinge line** of large anticlinal structure in hanging wall of Sibillini thrust

Violet:	Col 16
Purple:	Col 19
Light blue:	Col 7
Dark blue:	Col 17
Red:	Col 1
Brown:	Col 1b
Green:	Col 9
Yellow:	Col 3

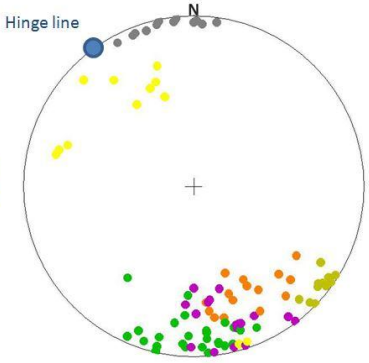

Figure 11c: Joints striking about **perpendicular to hinge line** of large anticlinal structure in hanging wall of Sibillini thrust

Purple:	Col 19a
Orange:	Col 1a
Yellow:	Col 18
Green:	Col 8
Light green:	Col 3a
Grey:	Col 2

Formation	Western limb, far from fold axis	Western limb, near fold axis	Eastern limb	Eastern limb overturned sector	Footwall
Turbidities					- Transversal joints (Col 18)
Bisciaro	- Stylolites parallel to hinge line (Col 2a) - Transversal joints (Col 2)				- Stylolites parallel to hinge line (Col 15a)
Scaglia Rossa	- Stylolites parallel to hinge line (Col 14)		- Stylolites parallel to hinge line (Col 10a) - Longitudinal joints (Col 10)		- Stylolites parallel to hinge line (Col 4)
Maiolica		- Longitudinal joint set (Col 1 and 1b) - Transversal joints (Col 1a)	- Longitudinal joint set (Col 7 and 17)	- Longitudinal joint set (Col 16 and 19) - Transversal joints (Col 19a)	
Calcari Diaspirini		- Longitudinal joints (Col 3) - Transversal joints (Col 3a)			
Calcare Massiccio		- Longitudinal joints (Col 9) - Transversal joints (Col 8)			

Table 2: Overview of the facture sets found at the digitized outcrops

Longitudinal joints

The longitudinal joints are nearly bedding-normal, as can for instance be seen in the corresponding Wulff net plots of Col 3 and Col 9 in Figure 12.

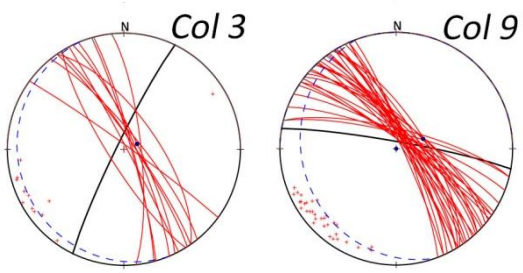

Figure 12: Stereoplots of the Calcari Diasprigni Fm, western limb near fold axis (Col 3) and Calcare Massiccio Fm, western limb near fold axis (Col 9). The longitudinal joints (red) are oriented perpendicular to bedding (blue). The line in black represents the orientation of the outcrop surface.

Within the group of longitudinal joints, the fracture sets in the Maiolica Fm are striking. These are namely present in two sets instead of one, oriented symmetrically around the hinge line, as shown in Figure 13.

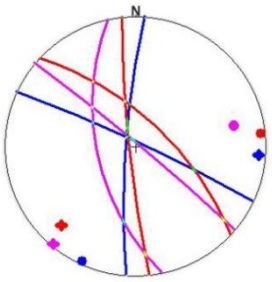

Figure 13: Two longitudinal fracture sets found in the Maiolica Fm. Red: eastern limb, overturned (Col 16, Col 19); blue: eastern limb (Col 7, Col 17); violet: western limb near fold axis (Col 1, Col 1b)

Deviating fracture sets

A few outcrops containing fracture sets that do not correspond to one of the three groups mentioned above are encountered. These are fracture sets Col 5 and 5a in the Calcare Massiccio Fm and Col 12 and 13 in the turbidite deposits in the western limb far from the fold axis, Col 6 and 6a in the Calcari Diaspirini Fm in the eastern limb, and finally Col 15 in the Bisciaro Fm in the footwall of the Sibillini thrust (Fig. 14).

Notable is that in the outcrops where Col 5 and 5a, Col 6 and 6a and Col 12 and 13 are digitized the orientation of the bedding is not in line with the NNW striking hinge lines of the anticlinal structures in the hanging wall and in the footwall of the Sibillini thrust. The correlation of these fracture sets with the hinge line will be discussed further in paragraph 3.1.2. (Interpretations).

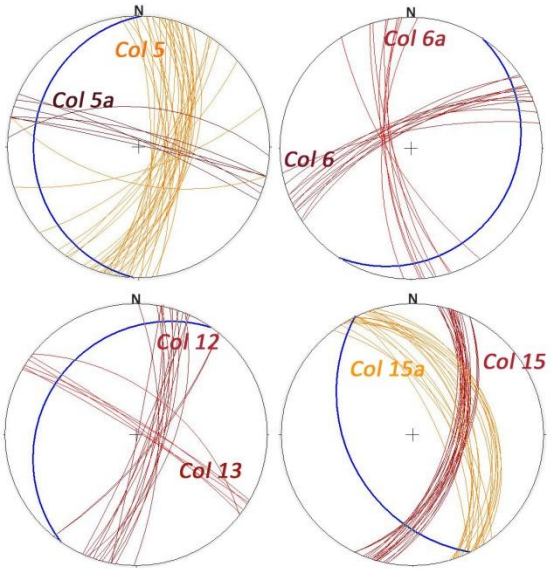

Figure 14: Stereoplots of outcrops with deviating orientations. The Calcare Massiccio Fm, western limb far from fold axis (Col 5 and 5a); Calcari Diasprigni Fm, eastern limb (Col 6 and 6a); Tubidites, western limb far from fold axis (Col 12 and 13) and Bisciaro Fm, footwall (Col 15 and 15a).
Legend: bedding: blue, joints: red and stylolites: orange

Minor folds and conjugate sets

In Col 4, fold structures of about 8 meters wide are present (Fig. 15). The fold axis of these folds is roughly parallel to the regional fold axis.

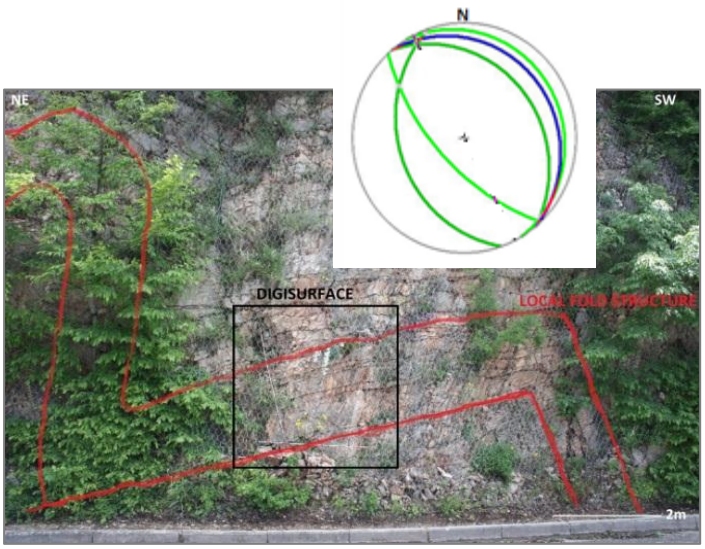

Figure 15: Minor fold structures in the Scaglia Rossa Fm on the footwall (Col 4). The digitized surface is denoted in black. The stereographic projection shows the orientation of the limbs of the local folds in green and the bedding in blue.

Bed-parallel stylolites

In some outcrops, bed-parallel stylolites were present. However, these are out of the scope of this research, because they most likely developed within a gravity-only scenario before the development of the fold-and-thrust belt. These are therefore not related to the stress regime corresponding to the fold-and-thrust belt.

3.1.2. Interpretations

We interpret the different fracture groups as the result of different structural stages of folding, shown in Fig. 16. We will place the fracture sets along with the other minor structures found in the study area into a sequence with three main stages (layer parallel shortening, folding and thrusting), as described by Tavarnelli (1997).

Stage 1: Layer parallel shortening

The earliest recognized stage of deformation is layer parallel shortening. This is mainly expressed by the development of bedding-normal pressure solution surfaces. We observed stylolites in the western limb far from the fold axis, the eastern limb and the footwall. This is in accordance with what is described by Tavani et al. (2012), namely that pressure solution surfaces develop mostly in the fold limbs (Fig. 17).

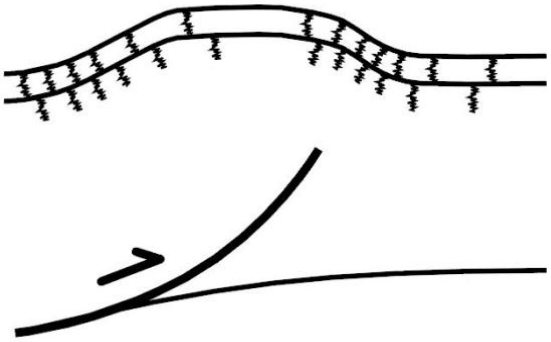

Figure 17: Expected stylolite pattern during early folding and thrusting. Stylolites mainly develop in the fold limbs (Tavani et al., 2012)

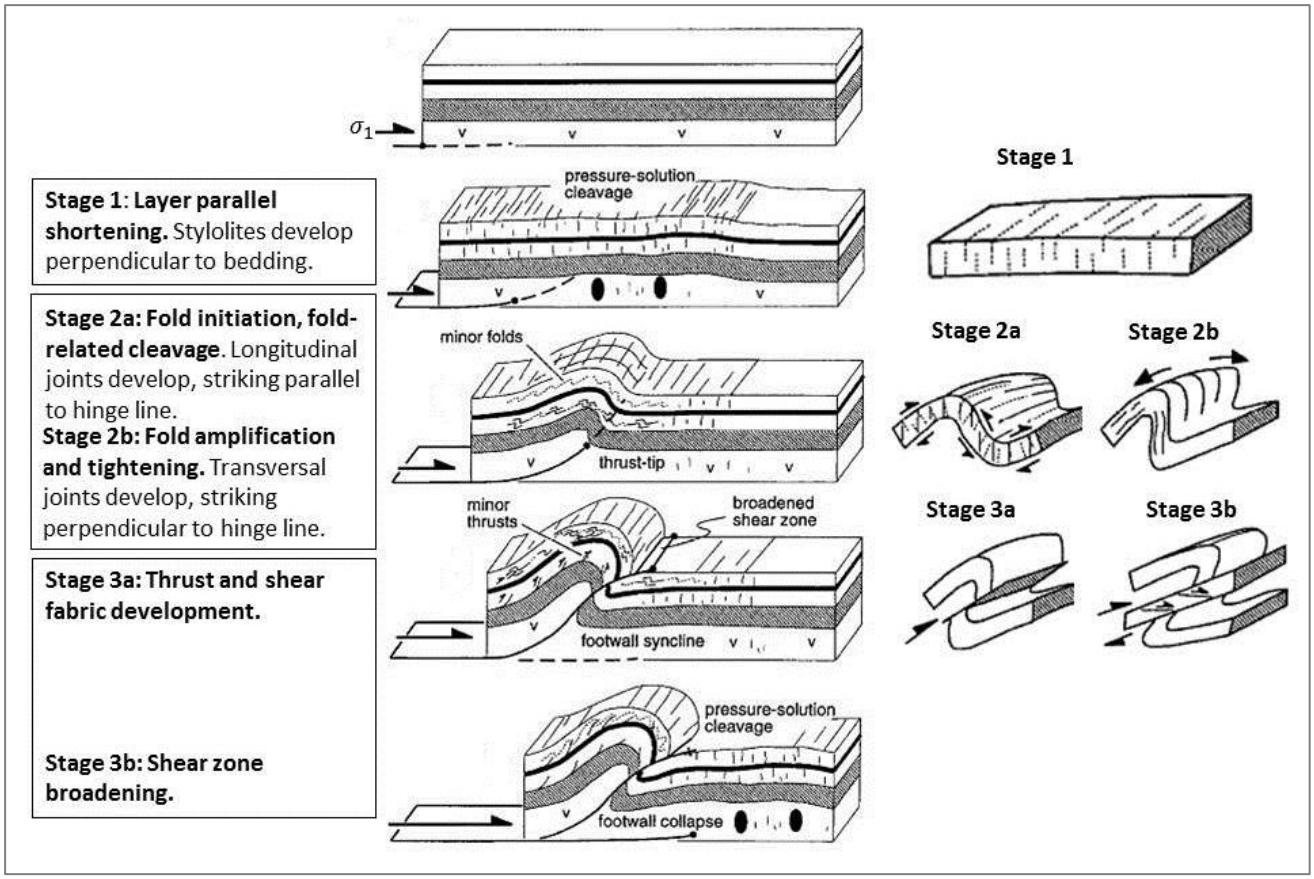

Figure 16: Structural stages of folding and thrusting, and related development of fractures. The model assumes gradual compressional deformation which progressively migrates from hinterland to foreland and kinematically linked folds and thrusts, the former growing ahead of the latter's terminations (Edited from Tavarnelli, 1997)

The average orientation of the different sets of stylolites after rotating the bedding to the horizontal is shown in Figure 18. It can be seen that the stylolites developed perpendicular to the main, NE directed principal stress. Col 4 and Col 10a deviate, having a dip angle significantly lower than 90°. This is possibly caused by locally deviating stresses or flexural slip.

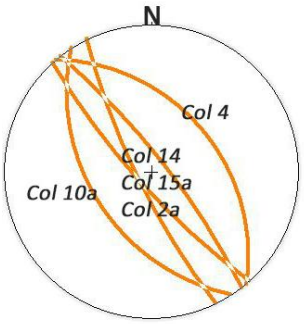

Figure 18: Stereographic projection of the stylolites after rotating the bedding to the horizontal. Every line represents the average orientation from the stylolites sets encountered in our study area

Stage 2: Folding

The second recognized structural stage is folding, during which the regional anticline developed.

Within the development of the large, regional anticline, smaller scale folds, defined as second- and third order folds, developed. Wavelength and amplitude of these folds range from centimeters to hundreds of meters. They were locally accompanied by the development of minor structures, such as joints and small faults, that sometimes overprinted earlier developed minor structures. The minor fold structures found in Col 4 (Fig. 15) are interpreted as these smaller-scale folds. The fact that the hinge line of these folds is parallel to the regional hinge line proves that these folds must have originated within the same stress regime as the regional fold.

The folding can be divided in two sub-stages, namely the initiation of the fold and the amplification and tightening of the fold.

Stage 2a: Fold initiation

Longitudinal joint origination

The longitudinal joint sets are interpreted as cleavage domains which originated during fold initiation. They are almost bedding-normal (Fig. 12, Table 3), and indicate a pattern which is convergent towards the inner arcs. Figure 19 *schematically* shows the orientation of the longitudinal joint sets within the limbs of the folds in our study area. This is accordance with literature (Tavani et al., 2012), but it must be noted that this interpretation is based on quite few data points and is therefore not decisive.

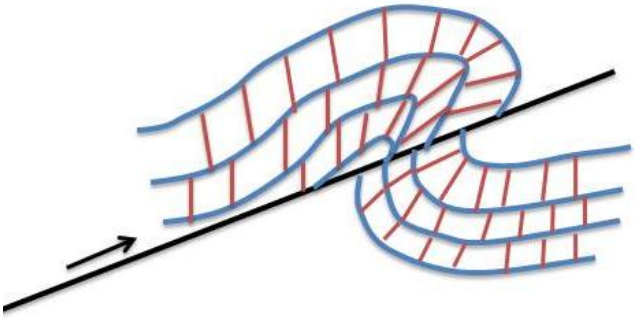

Figure 19: Schematic representation of longitudinal joint set pattern within the fold, the pattern is convergent towards the inner arcs

Formation	Angle between longitudinal joint and bedding
Turbidites, WL far	88° (Col 12)
Bisciaro, FW	81° (Col 9)
Calcari Diasprini, WL far	85° (Col 3)
Calcari Diasprini, EL	88° (Col 6)
Calcare Massiccio, WL near	82° (Col 9)

Table 3: Angle between longitudinal joints and bedding

Flexural slip

In the study area, bedding oblique stylolites striking about parallel to the hinge line are found (Fig. 20). These are interpreted as being tilted by flexural slip during folding. The tilting of the stylolites occurred within the regional compressional stress regime, shown by the fact that the intersection of the stylolites with the bedding is oriented about parallel to the regional hinge line.

In Col 4 the flexural slip is related to a small fold structure, stylolites and shear directions are indicated in Figure 21.

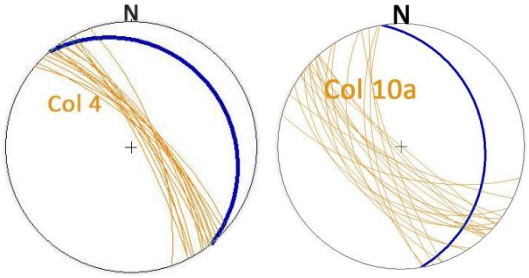

Figure 20: Stereographic projection of bedding oblique stylolites parallel to the hinge line, stylolites in orange and bedding in blue

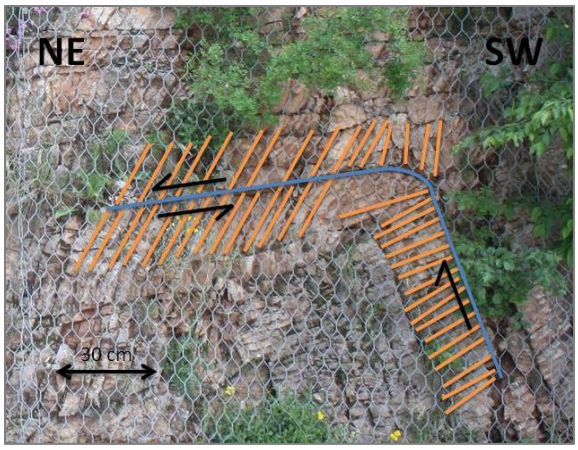

Figure 21: Flexural slip as a result of a local fold found in the Scaglia Rossa Fm on the footwall (Col 4)

Stage 2b: Fold amplification and tightening

Subsequently to fold initiation, fold amplification and tightening occur. The transversal joint sets are interpreted to have originated during this stage. A schematic overview of the acting principal stresses and the corresponding joints is shown in Figure 22.

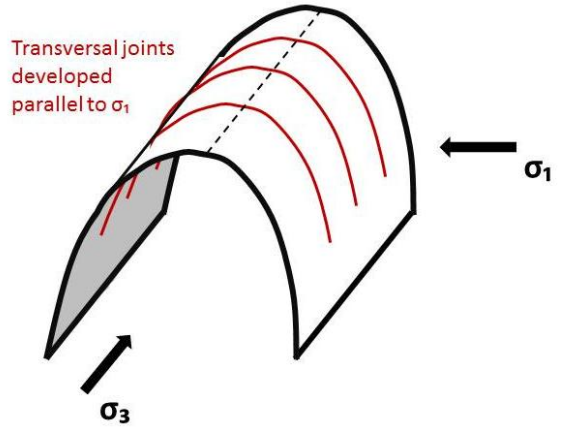

Figure 22: Schematic illustration of initiation of transversal joints as result of fold amplification and tightening (Constructed for this research)

Deviating fracture sets

A few outcrops contain fracture sets that do not correspond to one of the three groups mentioned above (Fig. 14).

These fracture sets are interpreted to have originated as hinge line parallel stylolites, longitudinal joints or transversal joints during the corresponding stages of folding, and to have been tilted by a different stress regime afterwards. This is indicated by the bedding orientation of these Cols, that is not in line with the hinge line of the large anticlinal structure in the hanging wall and the anticlinal structure of the footwall of the Sibillini thrust.

3.2. Geometry of fracture networks in correlation with lithology and tectonic position

In order to correlate the geometry of the fracture networks with lithology and tectonic position, 18 outcrops were digitized. A problem we encountered was that there was no suitable outcrop present in the study area for every combination of lithology and tectonic position, which is reflected in Table 4 and Table 5, where the densities [fractures/meter] and the fracture length [m] of the digitized outcrops are listed.

3.2.1. Fracture density

3.2.1.1. Observations

Table 4 displays an overview of the average fracture density and the standard deviation within all digitized surfaces.

Formation	Western limb, far from fold axis	Western limb, near fold axis	Eastern limb	Eastern limb, overturned sector	Footwall
Turbidities	1,5 ± 0,96 (Col 12) 0,29 ± 0,28 (Col 13)				0,73 ± 0,40 (Col 18)
Bisciaro	3,7 ± 2,0 (Col 2)				3,4 ± 3,7 (Col 15)
Scaglia Rossa	1,1 ± 0,37 (Col 14)		3,2 ± 1,0 (Col 10)		23 ± 3,9 (Col 4)
Maiolica		8,7 ± 2,2 (Col 1)	7,5 ± 2,4 (Col 7) 5,9 ± 4,0 (Col 17)	2,2 ± 1,1 (Col 16) 16 ± 4,3 (Col 19)	
Calcari Diaspirini		2,5 ± 0,67 (Col 3)	7,1 ± 2,9 (Col 6)		
Calcare Massiccio	9,0 ± 1,4 (Col 5)	4,4 ± 0,88 (Col 8) 2,1 ± 0,69 (Col 9)			

Table 4: Fracture densities given as average +/- standard deviation [fractures/meter]

Differences between tectonic positions

No clear, general relation between fracture density and tectonic position is observed.

Looking at the turbidite deposits and the Bisciaro Fm, fracture densities at the footwall seem slightly lower than those on the western limb (Table 4). However, the values lie closely together with relatively high standard deviations and are therefore not decisive.

In two outcrops, fracture sets are found with extremely high fracture densities: 23 on average in the Scaglia Rossa Fm on the footwall (Col 4, stylolites, Fig. 23) and 16 on average in the Maiolica Fm in the eastern limb, overturned sector (Col 19, transversal joints, Fig. 24).

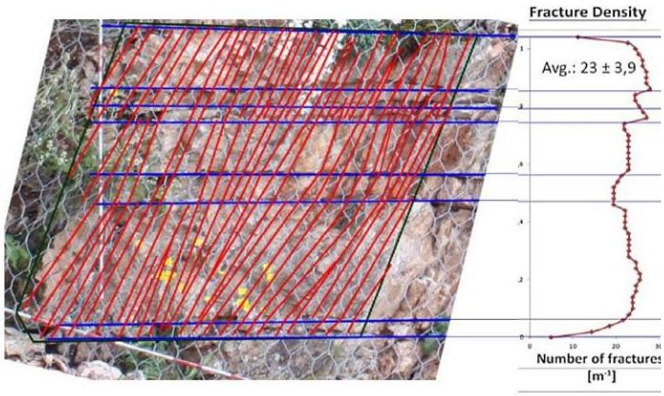

Figure 23: Col 4, Scaglia Rossa Fm in the footwall. The fracture density is very high, 23 per meter on average.

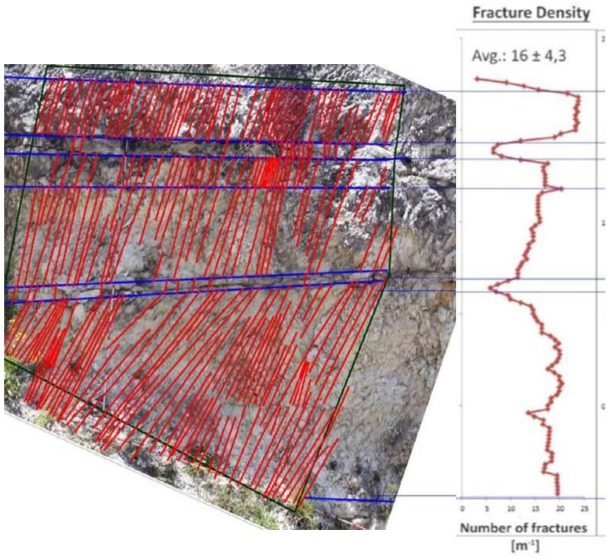

Figure 24: Col 19, Maiolica Fm on the eastern limb . The fracture density is very high, 16 per meter on average.

The longitudinal joint sets present in the Calcari Diaspirini in the western limb, near the fold axis (Col 3) have a larger spacing, hence a lower density than those in the eastern limb (Col 6) (Fig. 25).

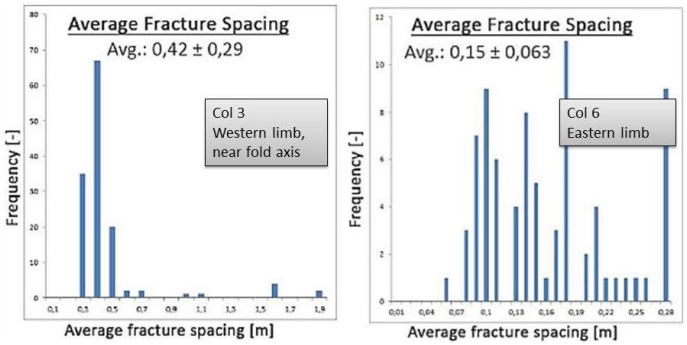

Figure 25: In the Calcari Diasprigni Fm, fracture spacing is larger in the western limb near the fold axis than in the eastern limb

Differences between different formations

With respect to differences in lithology, it is observed that the fracture sets in the turbidites generally have lower fracture densities than the carbonates and that among the carbonate deposits, the fracture density generally is highest in the Maiolica Fm (Table 4).

3.2.1.2. Interpretations

Differences between tectonic positions

No clear relation can be derived between tectonic position and fracture density, due to the limited amount of outcrops that was available.

The lower fracture density in the Calcari Diaspirini in the western limb, near the fold axis, compared to the eastern limb, is in accordance to literature. Namely, that in active hinge fault-related anticlines, fold limbs are preferred sites for deformation, rather than the corresponding anticlinal crests (Fig. 26) (Salvini, Storti, 2001; Salvini, Storti, 2004). However, we only have one formation in which we were able to digitize similar fracture sets in the same formation on the limbs as well as near the fold axis. Therefore there is no solid evidence to proof this theory.

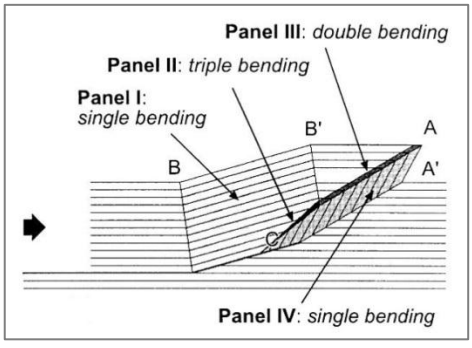

Figure 26: Schematic illustration of an overturned anticline upon a fault. Deformation takes place in fold limbs, rather than in the fold crest (Salvini, Storti, 2001)

The extremely high fracture density within the stylolites in the Scaglia Rossa Fm at the footwall (Col 4, Figure 23) is interpreted as being developed as the result of the formation of a smaller fold within the large anticline. In Figure 15 it can be seen that in this outcrop, the digitized surface (Col 4) is located on the north-eastern limb of a small fold of about 8 meters wide, that is visible in the outcrop along with another small fold which is about the same size.

The extremely high fracture density in the Maiolica Fm in the overturned sector (Col 19, Figure 24) is probably related to the fault damage zone. The fracture density within the Calcare Massiccio in the western limb, far from the fold axis, is higher than near the fold axis. This is in accordance with literature (Salvini, Storti, 2001; Salvini, Storti, 2004), that states that in active-hinge fault-related anticlines, fold limbs are preferred sites for deformation, rather than the corresponding anticlinal crests.

Differences between different formations

While subjected to the same deformation, fracture density in turbidites is generally lower than in the carbonate deposits. From this it can be interpreted that turbidite deposits are less sensitive to fracturing than carbonate deposits.

Fracture density is generally higher in the Maiolica Fm than in other formations. We think this is most likely related to the hardness of the rock, which in the field is observed to be high relative to the other formations.

3.2.2. Fracture height and termination

3.2.2.1. Observations

The fracture heights of all digitized outcrops are listed in Table 5.

Fracture height

The fracture height in the area generally varies between 15 cm and 1 m (Averages and standard deviations are listed in Table 5, detailed overview of fracture height within each Col in Appendices).

Striking is the fracture height of the Calcare Massiccio Fm, which is very high compared to the other formations at similar tectonic positions. The fractures within the Calcare Massiccio Fm almost always propagate through bedding boundaries (Fig. 27).

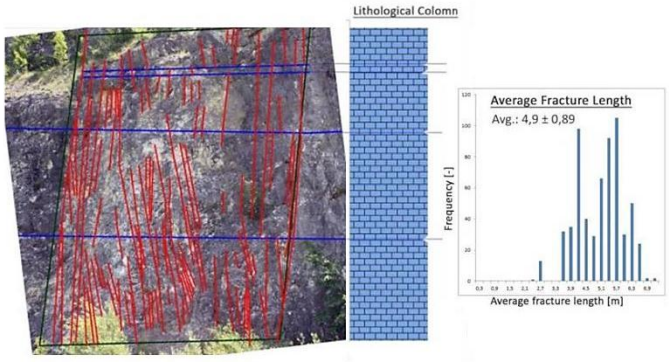

Figure 27: Col 9, Calcare Massicio Fm on the western limb near the fold axis. Fracture height is very high, fractures almost always propagate trough bedding boundaries

Fracture termination

Regarding fracture termination, several observations are made within the different formations.

In the Maiolica Fm and the Diasprini Fm chert is notably present in all outcrops, in the form of layers or lenses. Fractures almost always terminate on chert, causing chert layers to have a very low fracture density. Figure 28 shows for instance the fracture termination on chert within Col 17, the Maiolica Fm on the eastern limb.

Formation	Western limb, far from fold axis	Western limb, near fold axis	Eastern limb	Eastern limb, overturned sector	Footwall
Turbidities	1,3 ± 0,37 (Col 12) 0,46 ± 0,16 (Col 13)				0,94 ± 0,31 (Col 18)
Bisciaro	1,1 ± 0,40 (Col 2)				0,76 ± 0,23 (Col 15)
Scaglia Rossa	0,33 ± 0,085 (Col 14)		2,1 ± 0,65 (Col 10)		0,8 ± 0,11 (Col 4)
Maiolica		0,86 ± 0,14(Col 1)	1,6 ± 0,29 (Col 7) 0,31 ± 0,087 (Col 17)	0,38 ± 0,18 (Col 16) 0,53 ± 0,19 (Col 19)	
Calcari Diaspirini		1,5 ± 0,51 (Col 3)	0,57 ± 0,18 (Col 6)		
Calcare Massiccio	3,0 ± 0,28 (Col 5)	2,6 ± 0,28 (Col 8) 4,9 ± 0,89 (Col 9)			

Table 5: Fracture length given as average +/- standard deviation [m]

When looking at fracture termination apart from fracture termination on chert, it is observed that the fractures in the eastern and western limb in both of these formations are not particularly bed-confined, although bed-confined fractures do occur. This is visible in for instance Col 6, the Diaspirini Fm on the eastern limb (Fig. 29), and in Col 1 and 7 (Appendix A1 and A7 for more detail). In contrast with this are the Maiolica Fm outcrops in the overturned section of the eastern limb (Col 16 and 19), where nearly all fractures are bed-confined, as shown in Figure 30.

In the Bisciaro Fm the fracture density within the marl layers is very low, in contrast with abundant fractures within the limestone layers. In other words, fractures within the limestone layers terminate when encountering marl layers. This occurs in Col 2 and Col 15, Col 15 is shown in Figure 31.

In the turbidites most fractures terminate on bedding boundaries, although there are also fractures that terminate within a bedding. No clear cause for the termination of fractures within a bedding is observed.

3.2.2.2. Interpretations

The very high fracture height within the Calcare Massicio is most likely related to bedding thickness, which is very high in comparison with the other formations. Bedding thickness is around 5 m in the Calcare Massicio Fm, whereas bedding thickness in the other formations generally varies from 20 cm up to 1 m (See Appendices for details). Another factor in the large fracture height is the fact that fractures within the Calcare Massicio almost always propagate through bedding boundaries (Fig. 27).

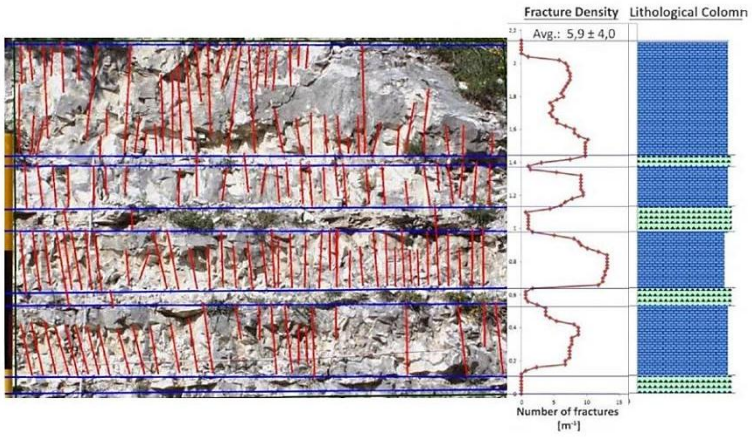

Figure 28: Fracture termination on chert layers in the Maiolica Fm (Col 17)

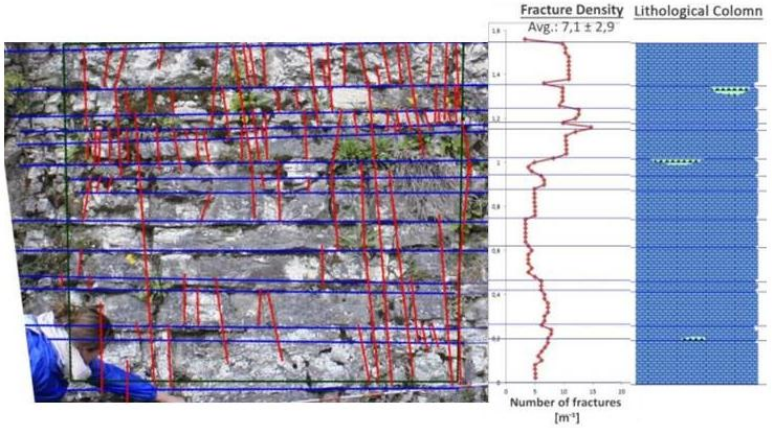

Figure 29: Col 6, Diaspirini Fm on the eastern limb. Bedding-confined fractures as well as unconfined fractures are present in the formation

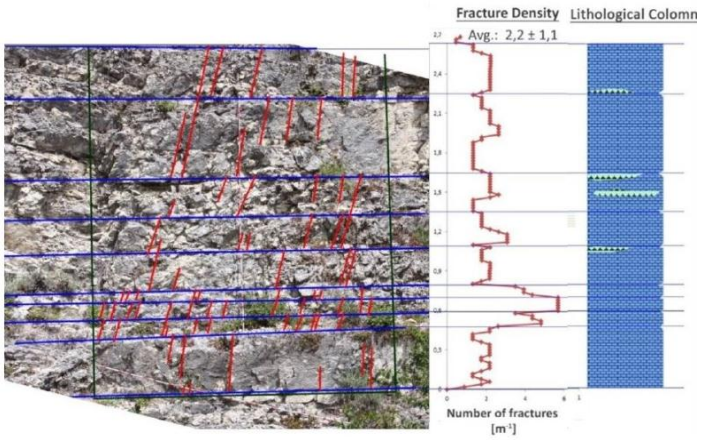

Figure 30: Col 16, Maiolica Fm in the overturned sector of the eastern limb. Almost all fractures are bedding-confined, independent of the presence of chert.

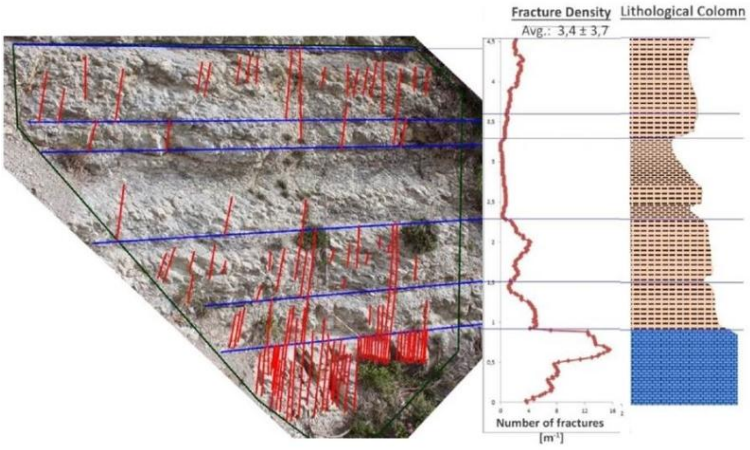

Figure 31: Col 15, Bisciaro Fm on the footwall of the Sibillini thrust. Fracture density in the limestone layers is very high, compared to the density in the marl layers.

Chert is interpreted as a non-fractured or very low fracture density-boundary between fractured beddings, that occur primarily in the Diasprini Fm and the Maiolica Fm.

Marl layers, present in the Bisciaro Fm, have a very low fracture density compared to limestone layers. We interpret this difference as the result of discrete deformation within the limestone layers and continuous deformation within the marl layers.

The cause of the termination of fractures on bedding boundaries within the Maiolica Fm in the overturned sector of the eastern limb lies probably in the overturning. It is interpreted as the result of shear in between layers, taking place during this phase of deformation.

Conclusion

The origination of a fold-and-thrust belt can be divided in structural stages, in which fractures and other minor structures such as minor folds develop within the larger fold-and-thrust structure. The orientation of the fractures is related to the structural stage in which they developed. The first stage is layer parallel shortening, during which bedding-normal pressure-solution surfaces develop perpendicular to the main principal stress. Subsequently, longitudinal joints striking parallel to the hinge line develop during fold initiation. This is followed by amplification and tightening of the fold, causing development of transversal joints, striking perpendicular to the hinge line.

In theory, fold limbs are preferred sites for deformation within an active-hinge fault-related anticline, rather than the corresponding anticlinal crests (Salvini, Storti, 2001; Salvini, Storti, 2004). Our data does not contradict to this, but is not substantial to proof this either.

Development of minor folds within the larger fold-and-thrust fold structures locally causes higher fracture densities.

Chert, primarily present in the Maiolica Fm and the Diasprini Fm, and marl, present in the Bisciaro Fm, act as non-fractured or very low density-boundary between fractured beddings.

Turbidites are less fractured than carbonates at similar tectonic positions.

Among carbonates, the Maiolica Fm has a relatively high fracture density, caused by the hardness of the rock. The fracture height in the Calcare Massiccio Fm is substantially higher than in the other carbonates, related to the high bedding thickness compared to the other formations.

Discussion

A problem we encountered in data acquisition is that there was no suitable outcrop present in the study area for every combination of lithology and tectonic position. Therefore it was not possible to draw conclusions about the correlation between fracture density and tectonic position.

For some of the combinations of lithology and tectonic position, suitable outcrops were only present in the study area far from the cross-section. Col 10 is located furthest away from the cross-section, namely 12 km. We assume that within the entire study area the same stress regime dominated. Still, the spreading in Col locations could cause errors because of local deviations in stress regime within the study area.

Another problem in acquiring data is related to the fact that a three-dimensional body is digitized using a two-dimensional picture. If multiple fracture sets are present within a rock, it is often the case that one of the fracture sets is oriented parallel to the outcrop surface. In order to be able to obtain a complete image of the fracture geometry of the outcrop, all fracture sets present have to be digitized. This means another outcrop, with a differently oriented outcrop surface, should be present at the same location. However, this occurs rarely.

The consequence of the inability to digitize all fracture sets within an outcrop is that it is not always possible to compare the geometry of the same fracture set (for example longitudinal joints) within different lithologies and tectonic position. It also has consequences for comparing fracture densities. Because in order to adequately compare fracture density, it should be done for the entire fracture geometry within a rock.

In the process of digitizing an outcrop, several sampling issues were encountered. Within an outcrop, it was not always possible to measure the orientation of the fracture planes in the upper part of the digitized surface. Furthermore, most of the outcrops did not have a smooth surface but were rather stumpy and curved. This causes fracture

planes to outcrop curvy, while they are actually straight lines. These fracture planes are drawn as straight lines.

Another difficulty arose in the process of locating and picking the Cols. This research is conducted in cooperation with Steenhuisen et al. (2013), and data acquisition is done simultaneously. Because fieldwork was done simultaneously, new insights in the geology of the study area arose during the process of data acquisition. Sometimes outcrops were already digitized before detailed cross-sections, leading to new insights in the geology, were finished. As a result of this some of the Cols had to be reassigned to different tectonic positions, creating gaps at other tectonic positions and thereby negatively influencing the possibility to compare different tectonic positions.

Recommendations

In order to overcome the problem of the limited amount of suitable Cols, we propose to enlarge the study area to an area that includes two fold-and-thrust structures in future research. In doing this more outcrops would be available per tectonic position (forelimb, backlimb, etc.) and a more adequate comparison could be made. It would be preferable to have detailed cross-sections at possible locations for Cols in advance, to be able to adequately pick locations to digitize outcrops.

If enough data could be acquired, it would be interesting to further test the theory that in active-hinge fault-related folding, the fold limbs are preferred sites for deformation rather than the corresponding anticlinal crest (Salvini and Storti, 2001; Salvini and Storti, 2004).

Several other subjects that would be interesting for further research are encountered in conducting this research. We found densities in the footwall that were slightly lower than the densities in the hanging wall, but differences were small. Exploring this difference further would be interesting.

Chert was present as a non-fractured or very low density-boundary between fractured beddings. It was primarily abundant in the Maiolica Fm and the Diasprini Fm. The presence of chert in a hydrocarbon reservoir would drastically lower the permeability in a hydrocarbon reservoir. Therefore it would be of interest to research what factors influence the development in chert in carbonate deposits and how the presence of chert could be predicted.

Finally, we found the longitudinal joints in the Maiolica developed as a two sets instead of one fracture set. In a hydrocarbon reservoir setting, this would highly enhance permeability. Hence, it would be interesting to find out what causes the joints to develop in two sets instead of one.

Acknowledgements

This work benefited from the good advice of prof. dr. Giovanni Bertotti. We thank Statoil for the fieldwork sponsoring.

References

Boncio, P., Lavecchia, G., 2000, A structural model for active extension in central Italy, Journal of Geodynamics, Vol. 29, page 233-244

Carminati, E., Lustrino, M., Doglioni, C., 2012, Geodynamic evolution of the central and western Mediterranean: Tectonics vs. igneous petrology constraints. In Tectonophysics 579 (2012), page 173–192

Di Naccio, D., Boncio, P., Cirilli, S., Casaglia, F., Morettini, E., Lavecchia, G., Brozzetti, F., 2005, Role of mechanical stratigraphy on fracture development in carbonate reservoirs: Insights from outcropping shallow water carbonates in the Umbria-Marche Apennines, Italy. In Journal of Volcanology and Geothermal Research 148 (2005), page 98-115.

Dürrast, H., Siegesmund, S., 1999, Correlation between rock fabrics and physical properties of carbonate rock reservoir rocks. In International Journal of Earth Sciences 88, page 392-408.

Gaetani M., 2010, From Permian to Cretaceous: Adria as pivotal between extensions and rotations of Tethys and Atlantic Oceans. In Journal of the Virtual Explorer, Vol. 36 .

Guenguen, E., Doglioni, C., Fernandez, M., 1998, On the post-25 Ma geodynamic evolution of the western Mediterranean. In Tectonophysics 298 (1998), page 259-269.

Guerrera, F., Tramontana, M., Donatelli, U., Serrano, F., 2012, Space/time tectono-sedimentary evolution of the Umbria-Romagna-Marche Miocene Basin (Northern Apennines, Italy): a foredeep model. In Swiss Journal of Geoscience (2012), Vol. 105, page 325-341.

Hancock, P.L., 1985, Brittle microtectonics: principles and practice. In Journal of Structural Geology, Vol. 7, page 437-457.

Hardebol, N.J., Bertotti, G., 2012, DigiFract: a software and data model implementation for flexible acquisition and processing of fracture data from an outcrop

Lemoine, M., 1982, Technical Report 42: Rifting and Early Drifting: Mesozoic Central Atlantic and Ligurian Tethys. In Deep Sea Drilling Projects and Publications, Volume 76, Part 6: Regional studies and geological models.

Marchegiani, L., Bertotti, G., Cello, G., Deiana, G., Mazzoli, S., Tondi, E., 1999, Pre-orogenic tectonics in the Umbria-Marche sector of the Afro-Adriatic continental margin. In Tectonophysics 315 (1-4), page 123-143.

Mazzoli, S., Deiana, G., Galdenzi, S., Cello, G., 2002, Miocene fault-controlled sedimentation and thrust propagation in the previously faulted external zones of the Umbria-Marche Apennines, Italy. In EGU Stephan Mueller Spec. Publ. Ser., 1, page 195-209.

Mazzoli, S., Pierantoni, P.P., Borraccini, F., Paltrinieri, W., Deiana, G., 2005, Geometry, segmentation pattern and displacement variations along a major Apennine thrust zone, central Italy. In Journal of Structural Geology 27 (2005), 1940-1953.

Salvini, F., Storti, F., 2001, The distribution of deformation in parallel fault-related folds with migrating axial surfaces: comparison between fault-propagation and fault-bend folding. In Journal of Structural Geology 23 (2001), page 25-32.

Salvini, F., Storti, F., 2004, Active hinge-folding-related deformation and its role in hydrocarbon exploration and development – Insights from HCA modeling, in K.R. McClay, ed., Thrust tectonics and hydrocarbon systems: AAPG Memoir 82, page 453-472.

Scarselli, S., G. D. H., Simpson, A., Allen, G., Minelli, Gaudenzi, L., 2007, Association between Messinian drainage network formation and major tectonic activity in the Marche Apennines (Italy), Terra Nova, Vol. 19, page 74–81

Scotese, C. R., 2001. Atlas of Earth History, Volume 1, Paleogeography, PALEOMAP Project, Arlington, Texas, 52 pp.

Sinclair, S.W., 1980. Analysis of Macroscopic Fractures on Teton Anticline, Northwestern Montana. MS Thesis, Department of Geology, Taxes A and M University.

Tavani, S., Storti, F., Bausà, J., Muñoz, J.A., 2012, Late thrusting extensional collapse at the mountain front of the Northern Apennines (Italy). In Tectonics, Vol. 31, TC4019.

Tavani, S., Storti, F., Salvini, F., Toscano, C., 2008, Stratigraphic versus structural control on the deformation pattern associated with the evolution of the Mt. Catria anticline, Italy. In Journal of Structural Geology, Vol. 30, Issue 5, page 664–681.

Tavarnelli, E., 1997, Structural evolution of a foreland fold-and-thrust belt: the Umbria-Marche Apennines, Italy. In Journal of Structural Geology, Vol. 19, Nos 3-4, page 523-534.